2021 43rd Annual International Conference of the
IEEE Engineering in Medicine & Biology Society (EMBC)
Oct 31 - Nov 4, 2021. Virtual Conference

2021 43rd Annual International Conference of the IEEE Engineering in Medicine & Biology Society (EMBC) | 978-1-7281-1179-7/21/$31.00 ©2021 IEEE | DOI: 10.1109/EMBC46164.2021.9629541

Design and Validation of a Sensor Fault-Tolerant Module for Real-Time High-Density EMG Pattern Recognition

Donald James Reynolds, *Member, IEEE*, Aashin Shazar, and Xiaorong Zhang, *Senior Member, IEEE*

Abstract— **With the advancements in electronics technology, high-density (HD) EMG sensing systems have become available and have been investigated for their feasibility and performance in neural-machine interface (NMI) applications. Comparing to the traditional single channel-based targeted muscle sensing method, HD EMG sensing performs a sampling of the electrical activity over a larger surface area and has the promise of 1) providing richer neural information from one temporal and two spatial dimensions and 2) ease of wear in real life without the need of anatomically targeted electrode placement. To use HD EMG in real-time NMI applications, challenges including high computational burden and unreliability of EMG recordings over time need to be addressed. This paper presented an HD EMG PR based NMI which seamlessly integrates HD EMG PR with a Sensor Fault-Tolerant Module (SFTM) which aimed to provide robust PR in real time. Experimental results showed that the SFTM was able to recover the PR accuracies by 6%-22% from disturbances including contact artifacts and loose contacts. A Python-based implementation of the proposed HD EMG SFTM was developed and was demonstrated to be computationally efficient for real-time performance. These results have demonstrated the feasibility of a robust real-time HD EMG PR-based NMI.**

I. Introduction

Electromyography (EMG)-based neural-machine interfaces (NMIs) have been studied and developed for decades to control neurorehabilitation systems such as neural prostheses which restore function for patients with limb loss or impairment [1]–[5]. The purpose of the EMG-controlled NMIs is to measure the muscle activities of relevant muscles, learn the patterns of collected EMG signals associated with different movement tasks, and make predictions of user's intended movement for control of external applications. With the advancements in electronics technology, high-density (HD) EMG sensing systems, which generally consist of 16 to 256 regularly spaced electrodes, have become available and have been investigated for their feasibility and performance in NMI applications [4], [6]–[8]. Comparing to the traditional single channel-based targeted muscle sensing method, HD EMG sensing performs a sampling of the electrical activity over a larger surface area and has the promise of 1) providing richer neural information from one temporal and two spatial dimensions [9] and 2) ease of wear in real life without the need of anatomically targeted electrode placement [6]. Some recent research findings have suggested that, comparing to traditional electrode placement method, HD EMG grids yield better robustness to electrode shift [10]–[12] and higher accuracy for EMG pattern recognition (PR) [4], [8], [13]. In addition, it opens possibility of directly extracting motor neuron spike trains for neurorehabilitation using HD EMG decomposition [9], [14]–[16].

To use HD EMG in real-time NMI applications, various methods have been explored to address the high computational burden associated with HD EMG sensing, including developing new computationally efficient features tailored to HD EMG [17], designing rapid EMG decomposition algorithms for real-time control of multi-degree-of-freedom systems [6], [16], [18], and employing parallel computing technologies such as FPGA and GPU to accelerate the processing of HD EMG signals [19], [20]. In our previous work, a novel spatial-temporal feature set named Adjacent Features (AFs) has been developed to analyze the intensity and structure of the HD EMG signals and the similarities between adjacent electrodes [17]. The experimental results showed that the developed AFs were not only computationally efficient for HD EMG PR; they also resulted in higher accuracies than Hudgins' time-domain (TD) features and autoregression (AR) based features for classifying various hand and wrist gestures [3].

Unreliability of EMG recordings over time is a challenge for applying EMG-based NMIs in practice. Conditions such as electrode shifts, movement artifacts, environmental noises, loose electrode-skin contacts, muscle fatigue, and arm posture may cause variabilities in the EMG characteristics and thus threaten the reliability of EMG-based control [21]–[23]. Although HD EMG has shown more robustness to electrode shift than traditional electrode placement method [10]–[12], its use in practice is still challenged by variances and disturbances such as movement artifacts and bad contacts, especially given that it is recording with many electrodes simultaneously without anatomically targeted electrode placement [24]. Our previous work has developed a Sensor Faculty-Tolerant Module (SFTM) for EMG PR systems and has tested it on single-channel EMG-based NMIs [25]. The SFTM consists of multiple sensor fault detectors and a self-recovery mechanism. The sensor fault detectors closely monitor the time-domain features of individual EMG signals to detect outliers, which are likely caused by disturbances. The self-recovery mechanism was developed by utilizing the information redundancy in multiple EMG signals. Our preliminary results have shown that removing one or two

This work is supported by the National Science Foundation (NSF #1752255).

The authors are with the School of Engineering at San Francisco State University, San Francisco, CA, 94132, USA. Corresponding author: Xiaorong Zhang; e-mail: xrzhang@sfsu.edu.

signals from the system will not significantly reduce the EMG pattern recognition performance. When disturbances are detected on certain EMG channels, the self-recovery mechanism will remove features of the "abnormal" signals from the system, retrain the classifier, and perform classification using features from "normal" signals only. The SFTM has great potential to perform well or even better in HD EMG based NMIs because a large number of signals will result in much more redundant information in the EMG recordings. This redundancy (using dozens or even hundreds of sensors) allows for selected electrode outputs which contain artifacts to be discarded while still providing the classifier with an overall view of muscle activity. By comparison, a sparse EMG array discarding faulty electrode signals during a localized physical disruption may be losing information on entire muscles' activity for the duration of the signal artifacts. In either case, gesture class separability is harmed by extracting features from artifacts or a critically incomplete electrode array.

This paper aimed to develop an SFTM for HD EMG PR based NMIs and evaluate its effectiveness on both commonly used TD and AR features as well as the newly developed AFs. A Python-based implementation of the proposed HD EMG SFTM was developed and tested on both normal EMG dataset and datasets contaminated by different types of disturbances. Performance metrics including the classification accuracy, system recovery performance, and CPU runtime were measured and analyzed.

II. Methods

A. Architecture of the HD EMG SFTM

Figure 1 shows the overall architecture of the proposed HD EMG PR based NMI, which consists of standard EMG PR modules coupling with the SFTM. The SFTM closely monitors the status of individual EMG input signals and responses accordingly to maintain system performance. The HD EMG input signals are preprocessed by amplifiers and filters and then segmented by overlapped sliding analysis windows. In each window, various features are extracted from each input signal and then fed to the SFTM. The signal fault detectors monitor the features of each EMG signal to detect anomalies. Based on the detection results, only the features extracted from normal channels are concatenated into a feature vector for pattern classification. If no anomaly is detected, the feature vector is directly sent to the classifier generated from the original training data. If one or more signals are determined as abnormal, a fast classifier retraining process is triggered and the feature vector derived from normal channels is fed to the new classifier for pattern classification.

Signal Fault Detector: A Mahalanobis distance analysis-based outlier detection method has been designed for individual HD EMG signal fault detection. We assume that disturbed signals are qualitatively different from EMG signals during normal motion activities. The detector is built only from normal training data without the need for prior knowledge of disturbed data. If a new piece of testing data has

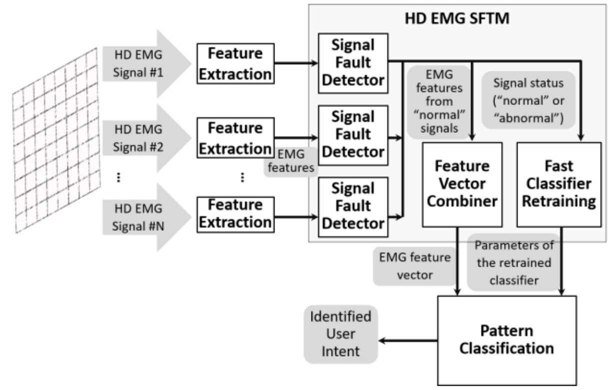

Figure 1. Overall system architecture of the HD EMG pattern recognition based NMI which consists of standard EMG pattern recognition modules coupling with the SFTM.

a large deviation from the normal EMG data, it will be flagged as a disturbance. The detector parameters can be calculated in the training procedure automatically. No more tuning step is required in the testing phase. More details of the signal fault detection algorithm can be found in [25].

Fast Classifier Retraining Process: For EMG PR-based NMIs, the original classifier will no longer be applicable when one or more EMG signals are removed from the system [5], [25]. The classifier needs to be retrained to recover the PR performance. The response time of the retraining algorithm is very critical to the design of real-time SFTM because the training process for HD EMG PR is time consuming due to the large amount of data produced. In our prior work, after examining the details of the linear discriminant analysis (LDA) algorithm, a computationally efficient classification algorithm that is commonly used in real-time NMIs, we have found that, by making efficient use of existing information obtained from the original training procedure, the LDA-based retraining procedure can be significantly simplified [25], [26]. The fast retraining algorithm can dramatically accelerates the retraining speed and is much more memory efficient compared to a full retraining process.

B. Feature Engineering

Both commonly used EMG features including TD features and AR coefficients and our newly developed spatial-temporal HD EMG AFs have been evaluated in this study.

TD Features: The Hudgins' TD features have been widely used in real-time EMG PR due to their low computational complexity and high accuracy [27]. The TD features used in this work include mean absolute value (MAV), root mean square (RMS), wavelength (W), zero crossings (Z), and sign slope changes (T).

AR Features: AR features are also commonly used because of their effectiveness in EMG PR [28]. In this study, the AR coefficients (denoted as AR_k, $k \in [0,5]$) and AR error (AR_e) of a sixth-order AR model have been included in our evaluation.

Adjacent Features: AFs have been developed in our prior work to analyze the intensity and structure of the HD EMG signals and the spatial relations between adjacent electrodes

[17]. The HD EMG signals are the result of motor unit action potentials (MUAP) propagating through the muscle tissues. Between adjacent channels, similarities in signal characteristics can be observed. The AFs approximate and quantify these characteristics by calculating the Mean Absolute Difference (MAD) between adjacent signals in the transverse (T) and longitudinal (L) directions. To calculate the AF, the transverse and longitudinal measured electrical signals (MESs) are shifted forward and backward by *dn* samples, and then compared to the reference MES. The MADs in the longitudinal and transverse direction of an electrode at the i, j location of the HD EMG grid are calculated as

$$MAD_{L,dn}[i,j] = \frac{\sum_{n=1}^{wl} |X_{i,j}[n] - X_{i+1,j}[n+dn]|}{wl} \quad \text{and}$$

$$MAD_{T,dn}[i,j] = \frac{\sum_{n=1}^{wl} |X_{i,j}[n] - X_{i,j+1}[n+dn]|}{wl},$$

respectively, where n is the sample within the analysis window, wl is the total number of samples in a window, dn is the number of samples to shift by, and $X_{i,j}$ is the normalized MES at the i, j location of the grid. In this study, six AFs have been evaluated including $MAD_{L,-1}$, $MAD_{T,-1}$, $MAD_{L,0}$, $MAD_{T,0}$, $MAD_{L,1}$, and $MAD_{T,1}$ because of their good performance in HD EMG PR based on our previous results [17].

Feature Engineering: A parameter tuning framework has been designed to optimize and identify the top performing feature sets. Specifically, three different parameter searches have been done in our experiments to investigate the following feature spaces:

- AFs only
- Combination of TD features and AR features
- Combination of AFs, TD features, and AR features

For each parameter search, up to three features are selected from each type of features (i.e., AFs, TD features, and AR features) to save time on tuning and to avoid computationally complex models.

C. System Implementation

The proposed real-time HD EMG SFTM was implemented based on Python 3 due to its low developmental complexity, high performance, high adaptability, portability, and library support. Key libraries including Numba and Intel oneAPI Math Kernel Library (MKL) were used in our implementation. Numba is a derivative of the NumPy scientific computing library that offers a Just-In-Time (JIT) compiler that translates a subset of Python code into super-fast machine code. The Intel oneAPI MKL accelerates linear algebra operations and routines. An open-source hyper-parameter optimization framework Hyperopt was used to develop our parameter tuning algorithm for the feature engineering phase [29].

D. Experiments

This study is conducted with Institutional Review Board (IRB) approval at San Francisco State University (SFSU) and informed consent of subjects. One male able-bodied subject was recruited. Data acquisition was conducted with the OT Bioelettronica's Quattrocento amplifier at 2560 samples per second with three surface EMG electrode grids (placed on the subject's dominate forearm) with 10mm spacing in an 8 by 8 arrangement, resulting in 192 channels.

Seven hand and wrist gestures including no movement, wrist supination, wrist pronation, hand close, hand open, wrist flexion, and wrist extension were performed in our experiments. The proposed HD EMG SFTM is not restricted to specific types of disturbances. To evaluate the performance of the SFTM, two common disturbances of EMG recordings have been investigated in this study: Contact Artifacts (CA) and Loose Contacts (LC) [21], [24]. In the CA trials, the seven gestures were made with a pen tapping on approximately the last 3 dozen electrodes (156-192) at a rate of 4-5 Hz. The exact electrodes affected vary from strike to strike. The LC disturbances were introduced with the last two rows of one 8x8 EMG electrode grid peeled back, and a towel placed between the electrodes and the skin while gestures were performed. Figures 2 and 3 show two representative trials of HD EMG signals contaminated by CA and LC, respectively.

In our experiments, three datasets were collected, including one normal EMG set, one set contaminated by CA, and one set contaminated by LC. For each dataset, the subject performed the seven gestures in sequence five times. Each gesture was performed for five seconds with short rest periods in-between. The sampled data were segmented into overlapped analysis windows with 100 ms length and 50 ms increment.

Evaluation of the effectiveness of the SFTM was based on the resulting accuracies from classification. To evaluate the

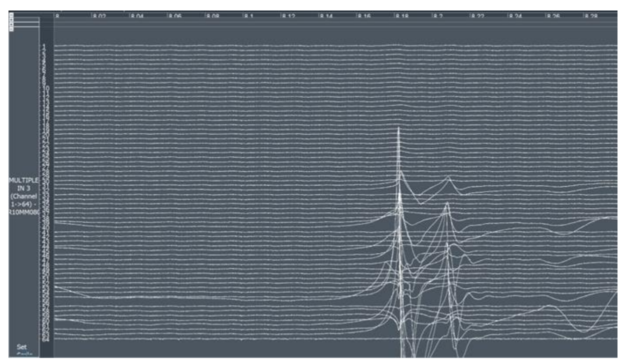

Figure 2. A representative trial showing HD EMG signals contaminated by CA

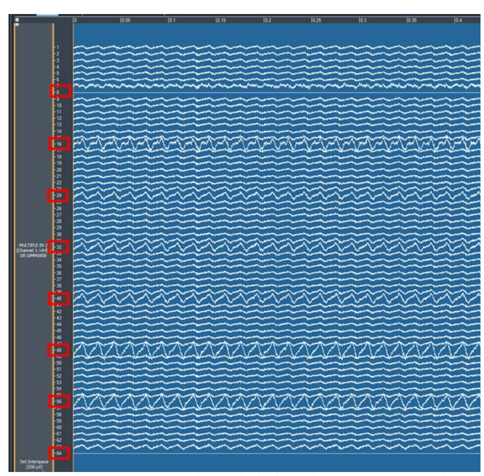

Figure 3. A representative trial showing HD EMG signals contaminated by LC

effect of the SFTM on EMG signals without disturbances, the normal EMG dataset was divided into five groups with each group containing one repetition of each gesture and then a five-fold cross validation was performed to calculate the averaged classification accuracy with and without the SFTM. For the CA and LC datasets, the normal dataset was used as the training set to create the initial LDA classifier and then the classification accuracies for the CA and LC datasets with and without the SFTM were calculated and compared.

The Python 3 based implementation of the HD EMG SFTM was running on a Huawei Matebook X Pro with an Intel i7-8550U CPU, 16GB of memory, and Windows 10 Home operating system.

III. Results and Discussion

Table I shows the classification accuracies of the HD EMG PR system with and without the SFTM on the CA and LC datasets. Six selected feature sets with highest overall recovered classification accuracies are included in this table. The positive effects of the SFTM are evident, increasing the classification accuracies by 6%-22%. All selected feature sets can recover the EMR PR performance to over 90% thanks to the SFTM. The benefit is the greatest when AFs are used where the recovered classification accuracies can be as high as 97%. This further proves the effectiveness and robustness of AFs in HD EMG PR. The computational requirements of AFs are comparable with those of TD features, which makes AFs effective features for real-time HD EMG PR systems.

Table I. Classification accuracy of the HD EMG PR system with and without the SFTM on CA and LC datasets

Features	CA w/o SFTM (%)	CA w SFTM (%)	LC w/o SFTM (%)	LC w SFTM (%)	Total w SFTM (%)
AF: $MAD_{L,-1}$, $MAD_{L,0}$, $MAD_{L,1}$	84.58	96.16	87.09	99.66	**97.91**
TD: Z, T **AR**: AR_3, AR_5 **AF**: $MAD_{L,-1}$, $MAD_{L,0}$	86.27	95.74	65.41	99.90	**97.82**
AF: $MAD_{L,-1}$, $MAD_{L,0}$	79.85	94.29	71.43	99.80	**97.04**
AF: $MAD_{L,0}$, $MAD_{L,1}$	77.59	93.94	82.41	99.36	**96.65**
TD: T **AR**: AR_2, AR_3, AR_4	76.19	84.46	96.34	99.25	**91.85**
TD: Z, T **AR**: AR_2, AR_3, AR_4	75.39	82.41	92.18	98.50	**90.45**

Table II. Classification accuracy of the HD EMG PR system with and without the SFTM on normal datasets

Features	Normal set w/o SFTM (%)	Normal set w SFTM (%)
AF: $MAD_{L,-1}$, $MAD_{L,0}$, $MAD_{L,1}$	100.00	100.00
TD: Z, T **AR**: AR_3, AR_5 **AF**: $MAD_{L,-1}$, $MAD_{L,0}$	100.00	99.90
AF: $MAD_{L,-1}$, $MAD_{L,0}$	100.00	100.00
AF: $MAD_{L,0}$, $MAD_{L,1}$	100.00	100.00
TD: T **AR**: AR_2, AR_3, AR_4	100.00	100.00
TD: Z, T **AR**: AR_2, AR_3, AR_4	99.95	99.90

Table III. SFTM CPU runtime with various configurations

# of abnormal Signals	SFTM CPU runtime (ms) with various number of extracted features				
	1 Feature	2 Features	3 Features	6 Features	9 Features
0	2.59	6.22	7.29	16.37	29.13
2	3.49	10.45	12.94	43.23	120.55
24	4.23	10.92	11.81	37.20	88.36
48	3.76	10.62	11.29	36.36	69.86
96	4.72	9.84	10.48	25.46	47.36
144	6.30	8.59	9.94	21.87	37.79
161	4.99	7.01	9.96	21.45	36.47
190	4.35	6.73	10.69	19.50	33.10

Table II shows the effect of the SFTM on the normal dataset with the six selected feature sets included in Table I. The results show that, for normal EMG data without disturbances, the SFTM only has slight effect on the PR performance. Only two feature combinations in Table II yield slightly lower (<0.1%) classification accuracies when SFTM is applied, which might be due to false detections from the signal fault detectors. Overall, the SFTM is effective in recovering HD EMG PR performance from disturbances and still maintains the PR performance when there is no disturbance.

Table III summarizes the CPU runtime of the Python-based SFTM implementation with various configurations based on two variables: 1) the number of signals detected as abnormal and 2) the number of features extracted for EMG PR. The SFTM process can be divided into a few major steps including feature normalization, feature reloading, fast retraining, and classification. The results show that the total SFTM CPU runtime for all configurations is less than 100 ms except for one configuration (2 abnormal signals and 9 extracted features). When six or fewer features are used, the CPU runtime for all configurations is less than 50 ms. This demonstrates the computational efficiency of the proposed SFTM and its promise in real-time HD EMG PR applications. With the assistance of GPU and other advanced computing techniques, the processing speed of the SFTM can be further accelerated.

IV. Conclusion

This project designed and validated an HD EMG PR based NMI which seamlessly integrates HD EMG PR with an SFTM that detects signal anomaly, retrains the classifier, and performs reliable PR in real-time. Three types of HD EMG features (TD features, AR features, and AFs) were evaluated on three datasets including a normal set and two contaminated sets with CA and LC, respectively. The SFTM was able to recover the classification accuracies by 6%-22%. The benefit of the SFTM was the greatest when AFs were used, which further proved the effectiveness and robustness of AFs in HD

EMG PR. A Python-based implementation of the proposed HD EMG SFTM was developed and was demonstrated to be computationally efficient for real-time performance. These results have demonstrated the feasibility of a robust real-time HD EMG PR-based NMI.

ACKNOWLEDGEMENT

The authors thank Justin Phan for his prior work and assistance in this study.

REFERENCES

[1] P. A. Parker and R. N. Scott, "Myoelectric control of prostheses.," *Crit. Rev. Biomed. Eng.*, vol. 13, no. 4, pp. 283–310, 1986.

[2] T. A. Kuiken *et al.*, "Targeted muscle reinnervation for real-time myoelectric control of multifunction artificial arms," *Jama*, vol. 301, no. 6, pp. 619–628, 2009.

[3] K. Englehart and B. Hudgins, "A robust, real-time control scheme for multifunction myoelectric control," *IEEE Trans. Biomed. Eng.*, vol. 50, no. 7, pp. 848–854, 2003.

[4] X. Zhang and P. Zhou, "High-density myoelectric pattern recognition toward improved stroke rehabilitation," *IEEE Trans. Biomed. Eng.*, vol. 59, no. 6, pp. 1649–1657, 2012.

[5] X. Zhang *et al.*, "On design and implementation of neural-machine interface for artificial legs," *IEEE Trans. Ind. Inform.*, vol. 8, no. 2, pp. 418–429, 2011.

[6] M. Ison, I. Vujaklija, B. Whitsell, D. Farina, and P. Artemiadis, "High-Density Electromyography and Motor Skill Learning for Robust Long-Term Control of a 7-DoF Robot Arm," *IEEE Trans. Neural Syst. Rehabil. Eng.*, vol. 24, no. 4, pp. 424–433, Apr. 2016, doi: 10.1109/TNSRE.2015.2417775.

[7] V. Glaser, A. Holobar, and D. Zazula, "Real-time motor unit identification from high-density surface EMG," *IEEE Trans. Neural Syst. Rehabil. Eng.*, vol. 21, no. 6, pp. 949–958, 2013.

[8] H. A. Jaber, M. T. Rashid, and L. Fortuna, "Using the robust high density-surface electromyography features for real-time hand gestures classification," in *IOP Conference Series: Materials Science and Engineering*, 2020, vol. 745, no. 1, p. 012020.

[9] M. Sartori, D. G. Llyod, and D. Farina, "Neural Data-Driven Musculoskeletal Modeling for Personalized Neurorehabilitation Technologies," *IEEE Trans. Biomed. Eng.*, vol. 63, no. 5, pp. 879–893, May 2016, doi: 10.1109/TBME.2016.2538296.

[10] A. Stango, F. Negro, and D. Farina, "Spatial correlation of high density EMG signals provides features robust to electrode number and shift in pattern recognition for myocontrol," *IEEE Trans. Neural Syst. Rehabil. Eng.*, vol. 23, no. 2, pp. 189–198, 2014.

[11] L. Pan, D. Zhang, N. Jiang, X. Sheng, and X. Zhu, "Improving robustness against electrode shift of high density EMG for myoelectric control through common spatial patterns," *J. Neuroengineering Rehabil.*, vol. 12, no. 1, pp. 1–16, 2015.

[12] J. He and X. Zhu, "Combining improved gray-level co-occurrence matrix with high density grid for myoelectric control robustness to electrode shift," *IEEE Trans. Neural Syst. Rehabil. Eng.*, vol. 25, no. 9, pp. 1539–1548, 2016.

[13] M. Jordanic, M. Rojas-Martínez, M. A. Mañanas, and J. F. Alonso, "Spatial distribution of HD-EMG improves identification of task and force in patients with incomplete spinal cord injury," *J. Neuroengineering Rehabil.*, vol. 13, no. 1, pp. 1–11, 2016.

[14] D. Farina and F. Negro, "Accessing the neural drive to muscle and translation to neurorehabilitation technologies," *IEEE Rev. Biomed. Eng.*, vol. 5, pp. 3–14, 2012.

[15] D. Farina *et al.*, "The extraction of neural information from the surface EMG for the control of upper-limb prostheses: emerging avenues and challenges," *IEEE Trans. Neural Syst. Rehabil. Eng.*, vol. 22, no. 4, pp. 797–809, 2014.

[16] A. K. Clarke *et al.*, "Deep Learning for Robust Decomposition of High-Density Surface EMG Signals," *IEEE Trans. Biomed. Eng.*, 2020.

[17] I. M. Donovan, K. Okada, and X. Zhang, "Adjacent Features for High-Density EMG Pattern Recognition," in *2018 40th Annual International Conference of the IEEE Engineering in Medicine and Biology Society (EMBC)*, 2018, pp. 5978–5981.

[18] D. Y. Barsakcioglu and D. Farina, "A real-time surface emg decomposition system for non-invasive human-machine interfaces," in *2018 IEEE Biomedical Circuits and Systems Conference (BioCAS)*, 2018, pp. 1–4.

[19] S. Tam, M. Boukadoum, A. Campeau-Lecours, and B. Gosselin, "A fully embedded adaptive real-time hand gesture classifier leveraging HD-sEMG and deep learning," *IEEE Trans. Biomed. Circuits Syst.*, vol. 14, no. 2, pp. 232–243, 2019.

[20] A. Boschmann, A. Agne, G. Thombansen, L. Witschen, F. Kraus, and M. Platzner, "Zynq-based acceleration of robust high density myoelectric signal processing," *J. Parallel Distrib. Comput.*, vol. 123, pp. 77–89, 2019.

[21] C. J. De Luca, L. D. Gilmore, M. Kuznetsov, and S. H. Roy, "Filtering the surface EMG signal: Movement artifact and baseline noise contamination," *J. Biomech.*, vol. 43, no. 8, pp. 1573–1579, 2010.

[22] R. H. Chowdhury, M. B. Reaz, M. A. B. M. Ali, A. A. Bakar, K. Chellappan, and T. G. Chang, "Surface electromyography signal processing and classification techniques," *Sensors*, vol. 13, no. 9, pp. 12431–12466, 2013.

[23] I. Kyranou, S. Vijayakumar, and M. S. Erden, "Causes of performance degradation in non-invasive electromyographic pattern recognition in upper limb prostheses," *Front. Neurorobotics*, vol. 12, p. 58, 2018.

[24] H. R. Marateb, M. Rojas-Martinez, M. Mansourian, R. Merletti, and M. A. M. Villanueva, "Outlier detection in high-density surface electromyographic signals," *Med. Biol. Eng. Comput.*, vol. 50, no. 1, pp. 79–89, 2012.

[25] X. Zhang and H. Huang, "A real-time, practical sensor fault-tolerant module for robust EMG pattern recognition," *J. Neuroengineering Rehabil.*, vol. 12, no. 1, pp. 1–16, 2015.

[26] X. Zhang, H. Huang, and Q. Yang, "Real-time implementation of a self-recovery EMG pattern recognition interface for artificial arms," in *2013 35th Annual International Conference of the IEEE Engineering in Medicine and Biology Society (EMBC)*, 2013, pp. 5926–5929.

[27] B. Hudgins, P. Parker, and R. N. Scott, "A new strategy for multifunction myoelectric control," *IEEE Trans. Biomed. Eng.*, vol. 40, no. 1, pp. 82–94, 1993.

[28] G. Hefftner, W. Zucchini, and G. G. Jaros, "The electromyogram (EMG) as a control signal for functional neuromuscular stimulation. I. Autoregressive modeling as a means of EMG signature discrimination," *IEEE Trans. Biomed. Eng.*, vol. 35, no. 4, pp. 230–237, 1988.

[29] J. Bergstra, D. Yamins, and D. Cox, "Making a science of model search: Hyperparameter optimization in hundreds of dimensions for vision architectures," in *International conference on machine learning*, 2013, pp. 115–123.